Transactions of the Materials Research Society of Japan 29[5] 2005-2008 (2004)

Effects of Composition on Microstructure and on Thermal Stability of Sn-Ag-In Lead-Free Soldered Joints

K. S. Kim[1], T. Imanishi[1], K. Suganuma[1], S.Kumamoto[2], and M. Aihara[2]
[1] Institute of Scientific and Industrial Research, Osaka University
Fax: 81-6-6879-8522, e-mail: kskimm12@sanken.osaka-u.ac.jp
[2] Harima Chemicals, INC.

The microstructural and mechanical properties of the Cu joints soldered with Sn-3.5wt%Ag-(0, 4, 8 wt%)In-0.5wt%Bi alloys were evaluated. All Sn-Ag-In alloys basically form granular type Ag-In intermetallic particulates at interfaces, and also form Sn-In phase in a solder layer. The thermal stability of the assembly with the Sn-Ag-In alloys and their Cu joints have been examined on heat-exposure endurance up to 150 °C. The interfacial phases of all Sn-Ag-In/Cu joints are typical Cu_6Sn_5 scallops. The interfacial layer and fine Ag-In intermetallic compound slightly grow by heat-exposure. As a result of heat-exposure at 100, 125, and 150 °C up to 1000 h, the shear strengths did not show any serious degradation for all joints.
Key words: lead-free, solder, Sn-Ag-In, microstructure, intermetallic compound

1. INTRODUCTION

The Sn-Ag-Cu ternary alloys are known to possess good solderability and mechanical property, and already have been widely used as reliable lead-free solder. There are, however, still some problems to be resolved for this alloy. Sn-Ag-Cu ternary alloy has higher melting temperature by about 34 °C than Sn-Pb eutectic alloy. Then this solder system requires higher temperature than typical Sn-Pb alloy for soldering. It is required to establish a certain kind of low temperature soldering techniques, especially for temperature-sensitive components, liquid crystal displays, optoelectronics modules, and thin printed wiring boards.

The low processing temperature is desirable for preventing electronic devices from heat damage during soldering processes and this gives a reason for the adoption of the other alloys, i.e., Sn-Zn-Bi, Sn-Ag-Bi, and Sn-Ag-In. The addition of In to Sn-Ag eutectic alloy can reduce its melting temperature effectively and can promote wetting on Cu [1, 2]. This alloy system can provide an excellent solution to those requirements mentioned above. Thus, Sn-Ag-In alloy has recently attracted considerable attention that can replace Sn-Pb eutectic solder without increasing soldering temperature. However, there are still unknown features on the effects of the addition of In to Sn-Ag eutectic alloy both on microstructural and mechanical properties. For soldering materials that must also give a structural integrity to electronics assemblies, one needs to understand the solidification phenomena in soldering, which can provide useful information to control microstructure.

Excess amount of In may degrade mechanical properties, particularly fatigue resistance, because a low-temperature soft phase is formed [3]. Thus, Sn-3.5wt%Ag-(0, 4 and 8)wt%In alloys were selected, and the microstructural change and shear tests of the solder joints after heat-exposure were examined. The purpose of the present work is also to clarify the solidification phenomena and the thermal stability of Sn-Ag-In alloys.

2. EXPERIMENTAL PROCEDURES

The three types of solder pastes, Sn-3.5wt%Ag -0.5wt%Bi, Sn-3.5wt%Ag-4wt%In-0.5wt%Bi and Sn-3.5wt%Ag-8wt%In-0.5wt%Bi, were supplied by Harima Chemicals, INC. The chemical compositions of Sn-Ag-In pastes are listed in Table 1. Hereafter, the composition unit "wt%" is omitted and they are simply called as Sn-3.5Ag-*x*In (*x*=0, 4 and 8). The melting

Table 1 Chemical composition of solder pastes (wt%).

	Ag	In	Bi	Pb	Sb	Cu	Sn
Sn-3.5Ag	3.51	0	0.49	0.03	0.01	0.003	Bal.
Sn-3.5Ag-4In	3.50	4.0	0.50	0.02	0.02	0.001	Bal.
Sn-3.5Ag-8In	3.50	8.0	0.52	0.02	0.02	0.001	Bal.

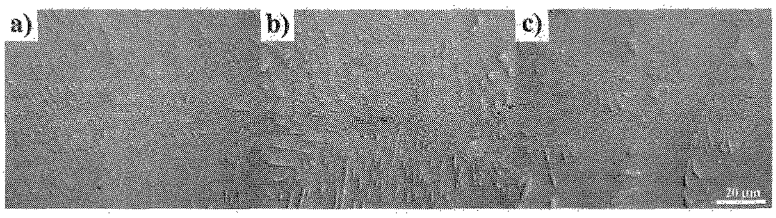

Fig. 1 SEM images of three alloys: (a) Sn-3.5Ag, (b) Sn-3.5Ag-4In, and (c) Sn-3.5Ag-8In.

reactions of the solder pastes were examined by using a differential scanning calorimeter (DSC). Dynamic scanning experiments were carried out on the solder samples of 10 mg to 20 mg in a temperature range from 30 °C to 300 °C at a heating rate of 5 °C/min. The samples were placed in aluminum pans and were scanned in an argon gas stream at 35 cc/min. Thermodynamic simulation assuming Scheil's solidification was carried out by using ThermoCalc with the Adamis7 database.

The solder pastes were printed onto glass-epoxy circuit boards (FR-4). Resistor chips (1608R) with Sn-10Pb plating termination were assembled on Cu pads on the FR-4. Reflow was carried out in air, and the peak temperature was 240 °C. After reflow treatment, heat-exposure test was carried out in air by putting the soldered joints into an oven. The joining samples were exposed at 100, 125 and 150 °C for up to 1000 hours. Joint strength was evaluated by a shear test. The shear test of the 1005R chip components on PWBs was carried out at room temperature by Dage Bondtester 4000. The shear speed was 500 µm/s.

Microstructures of the soldered samples were observed by optical microscope (OM), scanning electron microscope (SEM) and electron probe microanalysis (EPMA). The X-ray diffraction (XRD) analysis was also carried out.

3. RESULTS AND DISCUSSIONS

3.1 Microstructures of three alloys

The influences of alloy composition on as-reflowed microstructures are shown in Fig. 1. Sn-3.5Ag shows that eutectic fine Ag_3Sn/β-Sn phases form networks surrounding primary β-Sn grains of a few µm in size. For Sn-Ag-In alloys, fine precipitates are observed inside β-Sn grains, and particulate phases are also observed near the fine precipitates. For determination of the phases that appeared in these alloys, XRD analysis was carried out. Fig. 2 shows the typical XRD profiles for three alloys. In the case of Sn-3.5Ag alloy, the small peaks indicating only Ag_3Sn were detected with strong peaks of β-Sn phase as shown in Fig. 2(a). On the other hand, Sn-3.5Ag-4In and Sn-3.5Ag-8In alloys show the different small peaks, i.e., Ag_3In (ζ-(Ag-In)) phase. This phase shows similar peak positions to those of Ag_3Sn. From the EPMA maps, this phase contain both Ag and In as shown in Fig. 3. In the case of the Sn-3.5Ag-8In, $InSn_4$ (γ-InSn) peaks were also detected. Thus, it is apparent that Sn-Ag-In alloys form different IMCs after reflow treatment as compared with Sn-Ag.

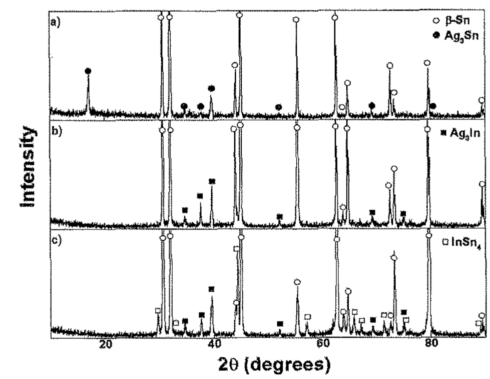

Fig. 2 XRD patterns from three alloys:(a) Sn-3.5Ag, (b) Sn-3.5Ag-4In, and (c) Sn-3.5Ag-8In.

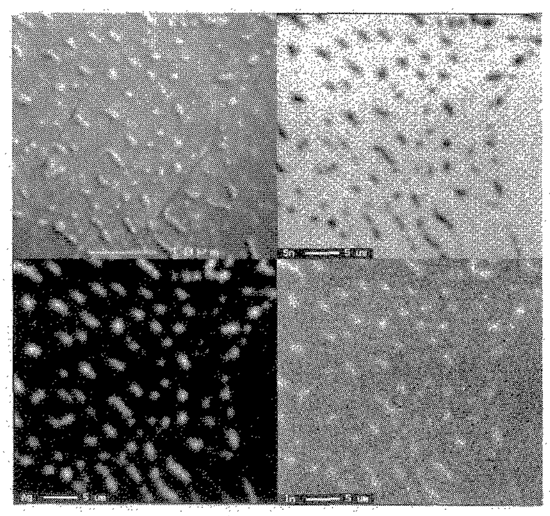

Fig. 3 SEM image and EPMA maps of Sn-3.5Ag-8In after reflow treatment.

3.2 Melting reaction

Typical DSC curves for the three alloys on heating near their melting temperatures are shown in Fig. 4. The large endothermic peaks of Sn-3.5Ag, Sn-3.5Ag-4In and Sn-3.5Ag-8In alloys appear at 222 °C, 214 °C and 208 °C, respectively. Increasing In content, the melting temperature decreases. The melting reactions of Sn-3.5Ag-8In alloy exhibited the shallow plateau extending to 215 °C from the on-set temperature (193 °C). To understand the effect of In on melting and solidification, thermodynamic simulation assuming Scheil's model was carried out by using ThermoCalc with the Adamis 7 database. Fig. 5 shows the relationship between temperature and weight fraction of solid for three solders. Sn-3.5Ag shows a typical binary eutectic reaction. On the other hand, the solidification reaction of Sn-3.5Ag-4In and Sn-3.5Ag-8In can be divided into several reaction schemes as listed in Table 2. According to results of simulation, Sn-3.5Ag-4In and Sn-3.5Ag-8In alloys form several Ag-In or Sn-In phases, and especially, do not form Ag_3Sn phase. The temperature range for the last part of solidification of Sn-3.5Ag-8In alloy is very steep and large as shown in Fig. 5. This explains why the DSC curve of this alloy shows broad endothermic peak.

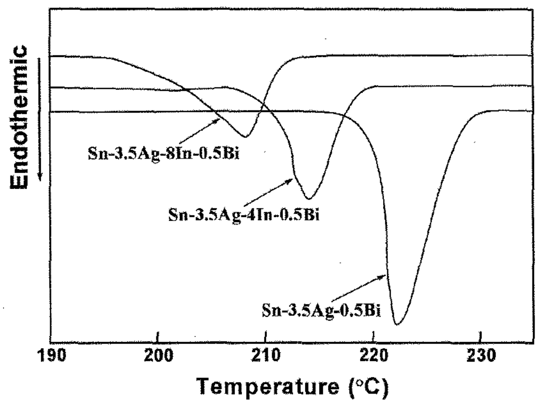

Fig. 4 DSC curves for the three solders on heating.

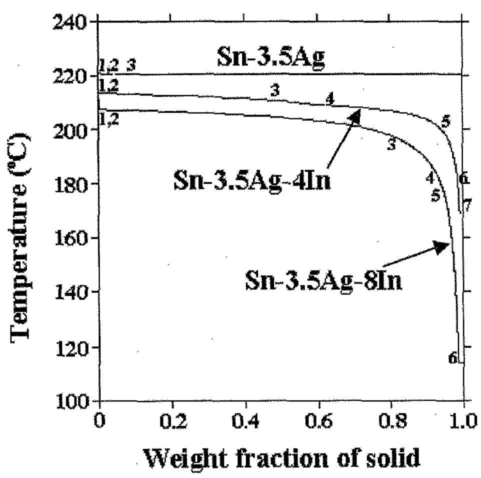

Fig. 5 Relationship between solid fraction-Temperature by Scheil's calculation by ThermoCalc with Adamis7.

3.3 Shear test of soldered joints

To investigate the effect of heat-exposure on the mechanical properties of the soldered joints, 1608R chip components were mounted on FR-4 boards and they were exposed at 100, 125 and 150 °C for up to 1000 h. Fig. 6 shows the interfacial microstructures of three Cu joints after reflow treatment. The reaction layer on a Cu pad is a typical Cu_6Sn_5 layer for three alloys.

Table 2 Reaction schemes of three alloys.

Sn-3.5Ag
1: Liquid
2: β-Sn, Liquid
3: Ag_3Sn, β-Sn, Liquid
Sn-3.5Ag-4In
1: Liquid
2: β-Sn, Liquid
3: β-Sn, ζ-(Ag-In), Liquid
4: β-Sn, ζ-(Ag-In), γ-InSn, Liquid
5: ζ-(Ag-In), γ-InSn, Liquid
6: Ag_2In, ζ-(Ag-In), γ-InSn, Liquid
7: Ag_2In, γ-InSn, Liquid
Sn-3.5Ag-8In
1: Liquid
2: ζ-(Ag-In), Liquid
3: ζ-(Ag-In), γ-InSn, Liquid
4: Ag_2In, ζ-(Ag-In), γ-InSn, Liquid
5: Ag_2In, γ-InSn, Liquid
6: Ag_2In, β-InSn, γ-InSn, Liquid

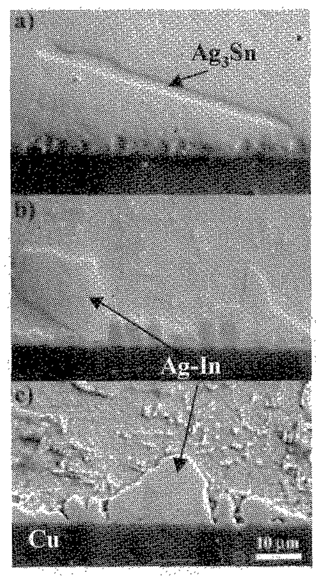

Fig. 6 Typical SEM images of three solder joints with Cu: (a) Sn-3.5Ag, (b) Sn-3.5Ag-4In, and (c) Sn-3.5Ag-8In.

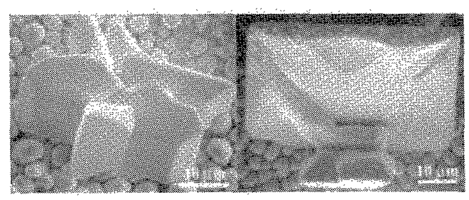

Fig. 7 SEM images of large Ag-In IMCs in Sn-3.5Ag-4In/Cu joint.

It is formed during reflow treatment, similar to the growth morphology in Sn-Pb/Cu and Sn-Ag based solders/Cu joints. Sn-3.5Ag-4In and Sn-3.5Ag-8In alloys frequently form large intermetallic grains, which was identified as An-In from EPMA, in addition to fine precipitates as shown in Fig. 7. The size of large Ag-In phase is larger than 20 μm. From the results of thermodynamic simulation, this large Ag-In phase can be ζ-(Ag-In) appeared as the primary phase on solidification. Fig. 8 shows the microstructure of solder/Cu pad interface before and after heat-exposure at 150 °C. The heat-exposure at all temperature in the present work enhances the growth of the reaction layer at the solder/Cu interface as well as coarsening of fine precipitates in a solder layer.

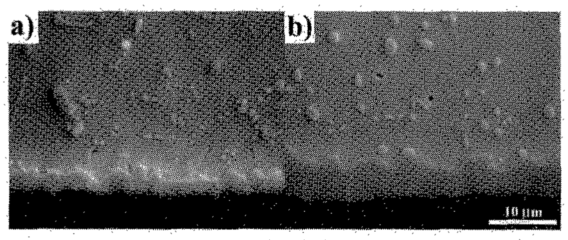

Fig. 8 SEM images of of Sn-3.5Ag-8In solder joints with Cu: (a) 0, and (b) 1000 h at 150 °C.

Fig. 9 shows the fracture patterns of the 1608R joints soldered with Sn-Ag-In. The fracture patterns can be categorized into four types, i.e., (a) cracking inside a chip (F1), (b) a chip/solder interface (F2), (c) inside solder (F3) and (d) along a Cu land/substrate interface (F4). Fig. 10 shows the incidence percent of each fracture pattern after 125 °C exposure. F3 is the most principal fracture pattern for all temperatures in the present work. Then, only F3 summarized the shear strength data at various temperatures as a function of heat-exposure time as shown in Fig. 11. The initial shear strengths of all soldered joints have almost the same values. The heat-exposure at 100, 125 and 150 °C up to 1000 h did not cause any serious degradation for all soldered joints. Thus, all the solder alloys with In addition up to 8 wt% can maintain good strength against heat-exposure.

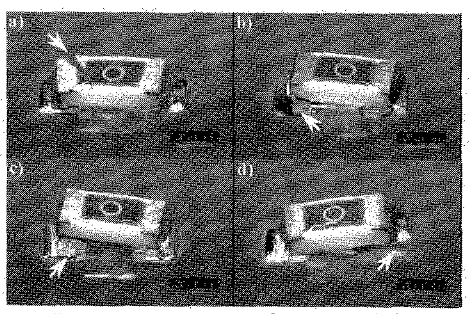

Fig. 9 Fracture patterns of 1608R joints after shear test: (a) cracking inside a chip (F1), (b) a chip/solder interface (F2), (c) inside solder (F3), and (d) Cu land/substrate interface (F4).

4. CONCLUSIONS

The present work examined microstructural and thermal behavior of Sn-Ag-In solders. The stability against heat-exposure of 1608R joints soldered with Sn-Ag-In was also investigated. The results can be summarized as:

1) The addition of In to Sn-3.5Ag causes the formation of granular type Ag-In intermetallic compound in the solder.
2) ThermoCalc calculation indicates that Sn-Ag-In alloys in the present work form several Ag-In or Sn-In phases. Large Ag-In particles appear in Sn-Ag-In solders on a Cu pad. They are formed along the interfacial reaction layer.
3) Heat-exposures from 100 to 150 °C do not have any significant influence on joint strength. The fracture of Sn-Ag-In soldered 1608R joints occurs inside of the solder layer.

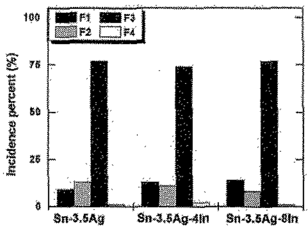

Fig. 10 Incidence percent of each fracture pattern after heat-exposure at 125 °C.

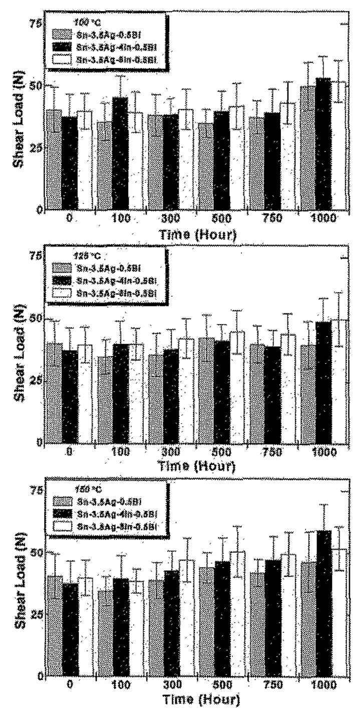

Fig. 11 Shear data of various solder joints.

5. ACKNOWLEDGEMENTS

The present work was performed under the support both of the Grant-in-Aid for Scientific Research (A) and of the 21COE program of The Japan Ministry of Education, Culture, Sports, Science and Technology in 2003.

6. REFERENCES

[1] P. T. Vianco and J. A. Rejent, *J. Electron. Mater.*, 28, 1138-1143 (1999).
[2] I. Artaki, A. M. Jackson and P. T. Vianco, *J. Electron. Mater.*, 23, 757-763 (1994).
[3] J. Hwang, *Surface Mount Tech.*, October, 1999.

(Received October 10, 2003; Accepted October 31, 2003)